Structural Engineering and Mechanics, *Vol. 58, No. 2 (2016) 379-395*
DOI: http://dx.doi.org/10.12989/sem.2016.58.2.379

Seismic performance of RC-column wrapped with Velcro

Minho Kwon[1a], Hyunsu Seo[1b] and Jinsup Kim[*2]

[1]*Department of Civil Engineering, ERI, Gyeongsang National University, Jinju 660-701, South Korea*
[2]*Department of Civil Engineering, University of Texas at Arlington, Arlington, TX 76019, USA*

(Received February 2, 2016, Revised March 11, 2016, Accepted March 15, 2016)

Abstract. A seismic strengthening method using Velcro is proposed to improve the seismic performance of columns in RC frame structures. The proposed method was evaluated experimentally using three fabricated RC specimens. Velcro was wrapped around the columns of the RC-frame specimen to prevent concrete spall falling. The reinforcing performance of the Velcro was determined from comparison of results on seismic performance (i.e., strength, displacement, failure mode, displacement ductility capacity and amount of dissipated energy). As the displacement of the reinforced specimens was increased, the amount of dissipated energy increased drastically, and the displacement-ductility-capacity of the reinforced specimens also increased. The final failure mode of RC frame structure was changed. As a result, it was concluded that the proposed seismic strengthening method using Velcro could be used to increase the displacement ductility of RC columns, and could be used to change the final failure mode of RC-frame structures.

Keywords: Velcro; RC column; seismic performance; concrete spalling; ductility

1. Introduction

In the last 50 years, there has been an increase in the number of destructive earthquakes (e.g., the 1967-Caracas earthquake, the 1968-Tokachi-Oki earthquake, the 1999-Izmit earthquake, the 2008-Wenchuan earthquake, the 2009-Honduras earthquake, and the 2011-Tohoku earthquake). During this interval, reinforced concrete (RC) buildings or infrastructure constructed in accordance with older seismic designs, have been severely damaged or completely destroyed (Priestley *et al*. 1996). A majority of these RC buildings collapsed due to column failure. Under seismic attack, columns of inadequate seismic design are particularly vulnerable since they are subjected to a complex combination of forces (axial load, flexure and shear, and possibly torsion). The collapse of a single column, or group of columns, can lead to at least partial collapse of a building. Following the increase in damage caused by severe earthquakes all over the world, there is great interest in effective seismic strengthening and retrofitting of older RC columns.

So far, many researchers have studied seismic strengthening and retrofitting of RC columns using external materials. Nowadays, steel-plate jacketing and continuous fiber sheet wrapping

---

∗Corresponding author, Ph.D., E-mail: jskim0330@gmail.com
[a]Professor, E-mail: kwonm@gnu.ac.kr
[b]Ph.D. Student, E-mail: flyfromyou00@gmail.com

http://www.techno-press.org/?journal=sem&subpage=8 ISSN: 1225-4568 (Print), 1598-6217 (Online)

have been used in seismic strengthening and retrofitting methods for existing RC columns. One well-known strengthening method involves used of steel jacketing in the plastic-hinge region of the RC column (Matsuda *et al*. 1990, Chai *et al*. 1991, Priestley *et al*. 1994, Xiao *et al*. 1996, Ha and Cho 2008). The steel-jacketing method could drastically enhance both the strength and ductility of RC columns. However, ease of construction or installation has driven researchers to search for alternative strengthening materials. Fiber-reinforced polymer (FRP) is a relatively new type of material used for external strengthening used in another well-known method: the fiber wrapping method (Priestley *et al*. 1991, Saadatmanesh *et al*. 1994, Saadatmanesh *et al*. 1996, Xiao and Ma 1997, Ascione and Feo 2000, Ye *et al*. 2003, Ascione *et al*. 2005, Aprile and Feo 2007, Lee 2007). For this, FRP is easily wrapped around the surface of existing structures by hand. A number of studies dealing with improved strength and ductility of confined concrete wrapped by prefabricated FRP jackets have also been carried out (Purba and Mufti 1999, Xiao and Wu 2003, Di Ludovico *et al*. 2008, Yan and Pantelides 2011, Kim *et al*. 2013). Some researchers proposed various approaches to predict FRP performance or failure. The stable numerical approach for anchorage reinforcing bar problem was proposed (Monti *et al*. 1997). Using such preliminary research, a noble mixed formulation to predict the bond-slip effect between FRP composite and concrete material was developed using a force-based approach (Limkatanyu and Spacone 2002). A simplified stochastic model was proposed to predict the strength distribution of single-ply unidirectional composites (Camata *et al* 2004a). Simple shear test and shear/normal test in bond failure tests were compared and used to investigate the relations between midspan debonding and end peeling failure through the experiments as well as numerical studies. (Camata *et al* 2004b).

Recently, new materials and products have been used to improve the seismic performance of RC columns. Aramid and vinylon continuous fiber ropes were used to improve column ductility (Shimomura *et al*. 2009). Vinylon and polypropylene fiber ropes were used as external confining reinforcements on standard concrete cylinders (Rousakis 2013, Rousakis 2014). A composite rope was used to confine a reinforced concrete column of square section (Rousakis and Tourtouras 2014). Polypropylene has a lower modulus of elasticity and ultra-high tensile deformation at failure, respectively. Columns wrapped with polypropylene fiber ropes did not reach fiber fracture. Continuous fiber ropes are easily arranged on the surface of existing structures by hand, and are used without epoxy resin. Moreover, such methods require no use of impregnating resins or mortar.

The application of Velcro to structural retrofitting is proposed in this paper. It consists of two components: one strip contains many small hooks; an opposing strip contains many small loops, as shown in Fig. 1. When the two components are pressed together, the hooks catch in the loops, and

(a) Hooks (b) Loops

Fig. 1 Components of Velcro

Fig. 2 Mushroom-shaped head hook of improved Velcro

Table 1 Physical properties of nylon

Weight (g/cm^3)	Tensile strength (kg/cm^2)	Elongation (%)	Rupture strength (kg/cm^2)
1.15	750	25	800~980

the two pieces become securely fastened until they are pulled apart. Therefore, in studies of Velcro, the focus has been on the adhesive force between the two components. In addition, the shapes of the Velcro hooks and loops have been refined to improve the adhesion between them.

The first Velcro was made of cotton. This material proved impractical and was replaced by nylon and polyester. Velcro fasteners made of Teflon loops, polyester hooks, and glass-fiber backing are used in aerospace applications (e.g., the space shuttles). Many new types of Velcro have been developed and are being produced. One new type uses a mushroom-shaped head as a hook (Fig. 2) that provides better adhesive force than typical Velcro. The mushroom-head-shaped hook is composed of polyester, and the normal-shape loop is composed of nylon. Velcro has the chemical, mechanical, and environmental resistance of the material from which it is fabricated; therefore, these are those of polyester and nylon. The basic physical properties of nylon are shown in Table 1. Moreover, Velcro can be applied to any shape of structure because of its flexibility.

In this study, a seismic reinforcement method using Velcro is proposed, to improve the seismic performance of RC frame structures. Velcro are wrapped the RC column to prevent concrete spall falling. The proposed method does not need corner treatment to make a round shape, although FRP confinement methods need corner treatment due to premature fracture of fibers at the corners prior to FRP activation or fragile failure would occur. Also, the proposed method does not need a bond material due to the self–anchoring characteristic of Velcro. The performance of Velcro for this purpose was evaluated experimentally after constructing three RC specimens. These RC specimens were half-size models of RC frame structures in an existing building. The Velcro was wrapped around the columns of the RC frame specimen.

2. Mechanical properties of Velcro

In this study, Velcro was used that consisted of both hooks and loops. Each Velcro tensile-test specimen was 200 mm long (pure test length: 100 mm), 50 mm wide, and 0.6 mm thick (thickness of each hook and loop was 0.3 mm). All tests were performed by displacement control and loading speed was 1 mm/min. The data sampling rate was 1.0 Hz. Both tensile strength and tensile

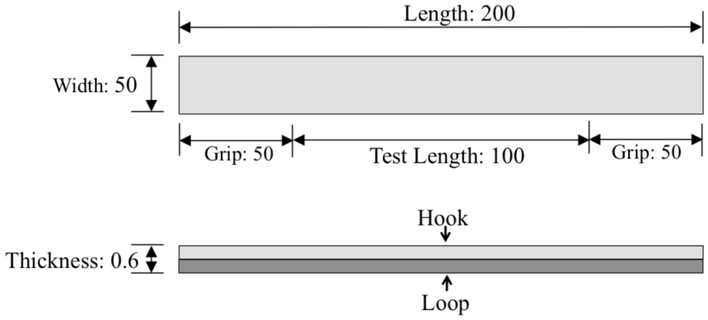

Fig. 3 Details of Velcro tensile-test specimens

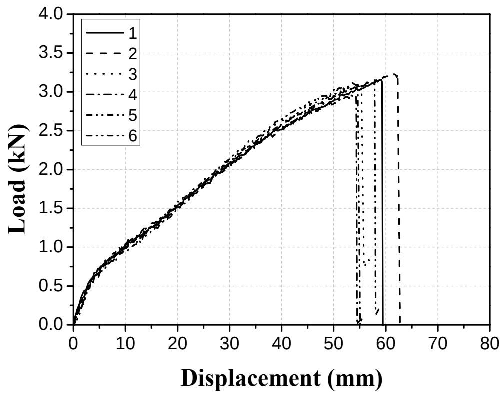

Fig. 4 Tension test results of Velcro tensile-test specimens

Table 2 Tensile test results of Velcro tensile-test specimens

Specimen	Max. Load (kN)	Max.Displacement (mm)	Deflection (%)	Elastic Modulus (MPa)
1	3.16	59.1	59.1	1266.8
2	3.24	62.3	62.3	1096.4
3	3.12	55.2	55.2	1249.7
4	2.97	54.3	54.3	1140.4
5	3.15	57.1	57.1	1140.0
6	3.12	53.6	53.6	1075.9
Average	3.13	56.9	56.9	1138.2

displacement of the Velcro tensile-test specimens were measured. The Velcro tensile-test specimens are illustrated in Fig. 3, and the tension test results are plotted in Fig. 4. The tension-test results are summarized in Table 2. The maximum tension load range of the Velcro tension-test specimen was from 2.97 kN to 3.24 kN and maximum displacement range was from 53.6 mm to 62.3 mm. Based on these results, the average maximum load and displacement were 3.12 kN and 56.9 mm, respectively. The average initial elastic modulus of the Velcro tensile-test specimen was 1138.2 MPa.

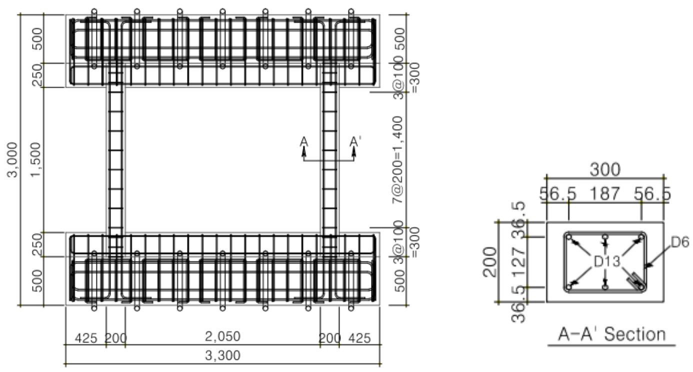

Fig. 5 Details of the RC specimens (unit=mm)

3. Experimental test

3.1 RC specimen

Three RC specimens were constructed for the experimental program. These RC specimens were half-scale models of RC columns in an old school building in Korea. The details of the RC specimens are depicted in Fig. 5. The total height and width of the RC specimens was 3,000 mm and 3,300 mm, respectively. The column height of the RC-frame was 1,500 mm and its cross-section 200×300 mm. The beam length of the RC-frame was 2,050 mm, and the beam cross-section was 150×250 mm. The RC-block dimensions were 750×500×3,300 mm, and were located at both the top and bottom of the RC-frame. The RC specimens were cast from ready-mixed concrete, for which the target compressive strength was 24 MPa. The average concrete compressive strength after 28 days (compression-test results) was 24.9 MPa. Six deformed D13-mm (13 mm diameter) rebars were erected for longitudinal reinforcement throughout a vertical member. Eight deformed D6-mm rebars were fastened at 200 mm spacing, in each of the RC columns for transverse reinforcement. The yield strength of all the deformed rebar was 400 MPa.

3.2 Details of the test specimens

The three RC specimens were used to test the reinforcement performance of the Velcro experimentally. The details of the test specimens were summarized in Fig. 6. The first RC specimen was an unaltered (original) specimen (ORC). The two other RC specimens were retrofitted with Velcro. One third of the column-length, at the top and bottom of the columns of the second RC specimen was retrofitted using Velcro to cover the plastic-hinge region (VQRC). The entire length of the column of the third RC specimen was retrofitted using Velcro (VARC). Fig. 7 presents the wrapping method of Velcro. Velcro was wrapped by hand using the self-anchoring characteristic of Velcro, so any bond material is not needed to install the Velcro. Corner treatment was not needed to make a round shape in concrete column section. As a result, Velcro is easy and fast to install. In this study, 500 mm width of hooks and 150 mm width of loops were used. Only one layer of Velcro, which is same as the Velcro tensile-test specimens, was installed. The hooks were located on the inside and the loops were located in outside. Each end was located in each loading direction surface.

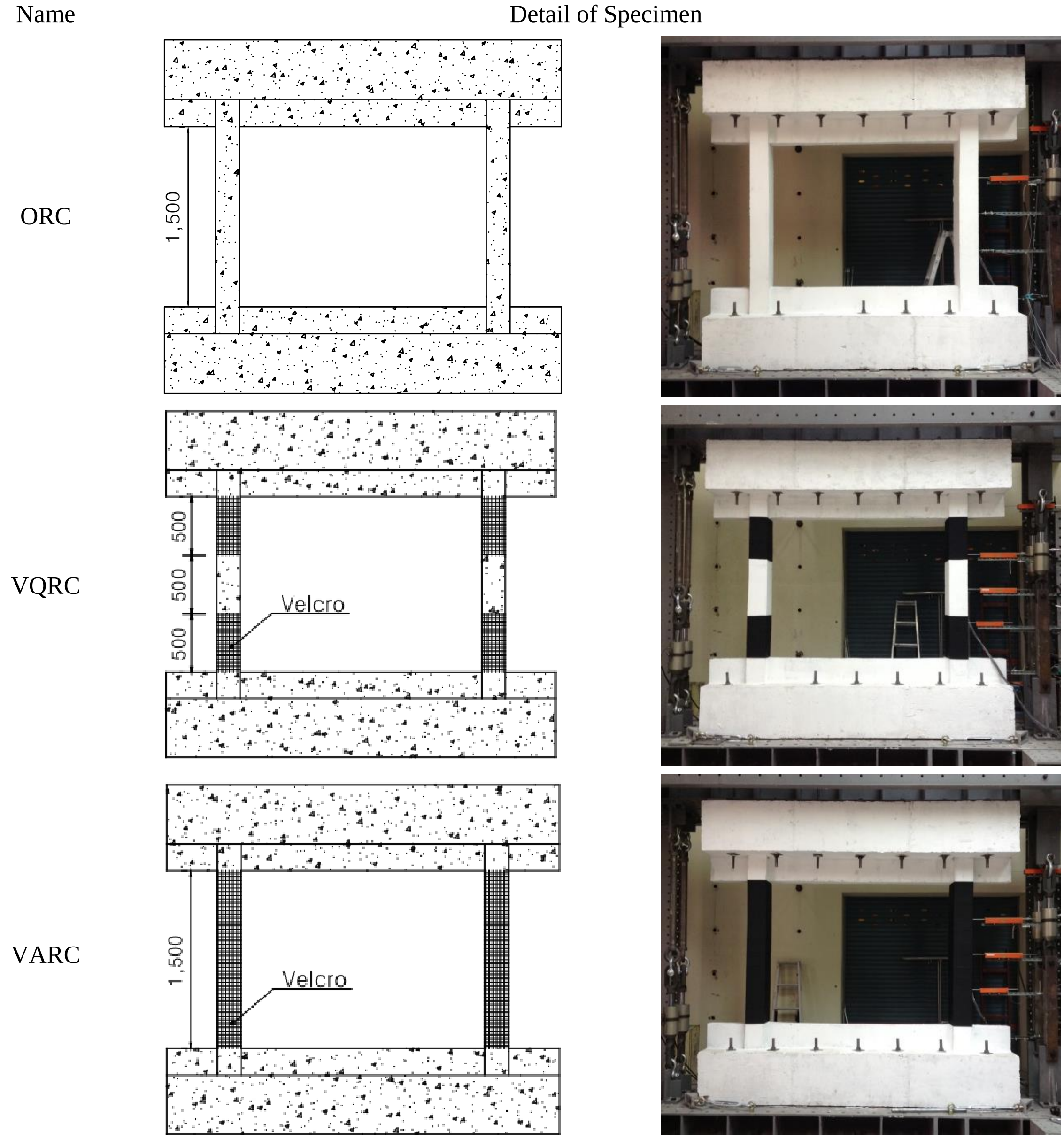

Fig. 6 Experimental details of the specimens.

3.3 Test setup

The test setup for the experiment is depicted in Fig. 8. The bottom block of the RC specimen was securely fastened to the reaction floor, and its top block was fixed to the loading frame. A 1000-kN hydraulic actuator was used to apply lateral displacement. The lateral displacements were imposed through the loading frame, that was supported by both four rollers and guide frames, fixed to the top block of the RC specimen. Four servo-type hydraulic jacks were used to load a

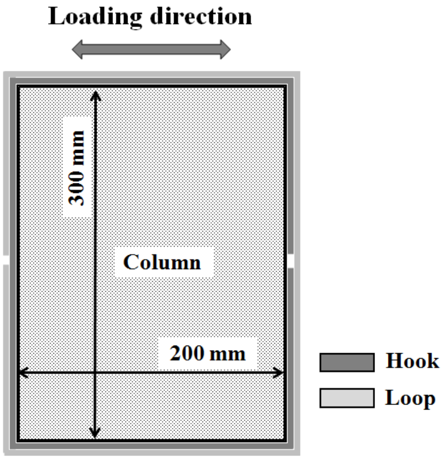

Fig. 7 Wrapping method of Velcro

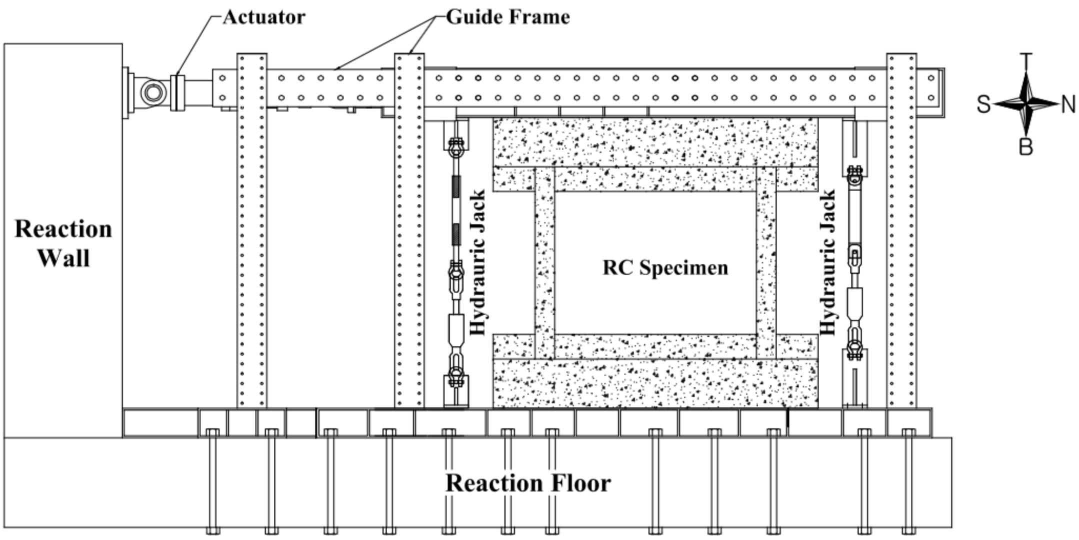

Fig. 8 Test setup

constant axial force of 288 kN (corresponding to approximately 0.1×Ag×fck, (Kim *et al*. 2013).

Fig. 9 shows the instrumentation plan of the strain gauges and LVDT. Five LVDT were installed in the right column at intervals of 375 mm. Four longitudinal rebars were located in the corners of the column cross-section, and each rebar had seven strain gauges attached. In addition, twelve strain gauges were attached at the stirrup.

3.4 Loading protocol

A quasi-static cyclic load established by lateral displacement, was used in the experiment to test the RC specimen. The lateral displacement load was increased by 5 mm to define the yield

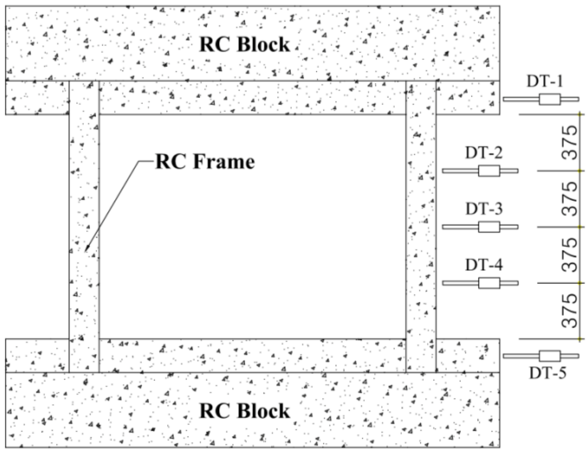

(a) L.V.D.T.

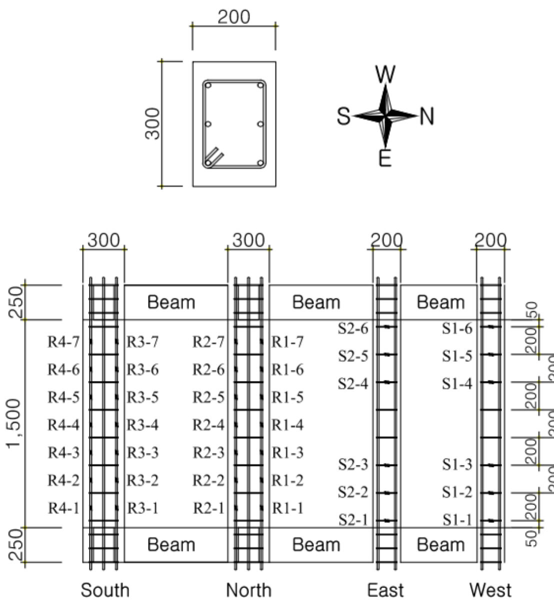

(b) Strain Gauge

Fig. 9 Instrumentation (unit=mm)

displacement point initially. The displacement ductility was determined from the first-yield displacement. After the displacement ductility was defined, the lateral displacement was loaded. The displacement ductility was increased by 0.5-displacement ductility at each loading step. Fig. 10 shows the loading protocol history.

4. Results and discussion

4.1 Failure mode

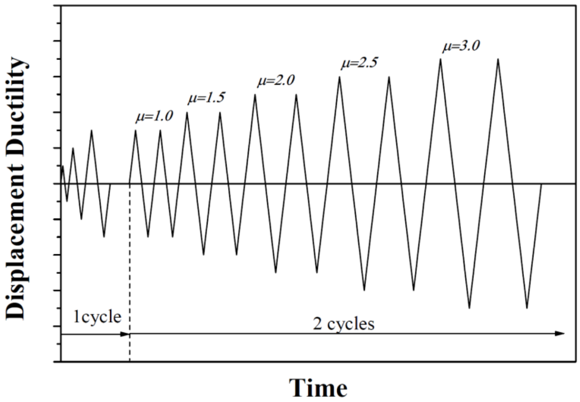

Fig. 10 Loading protocol

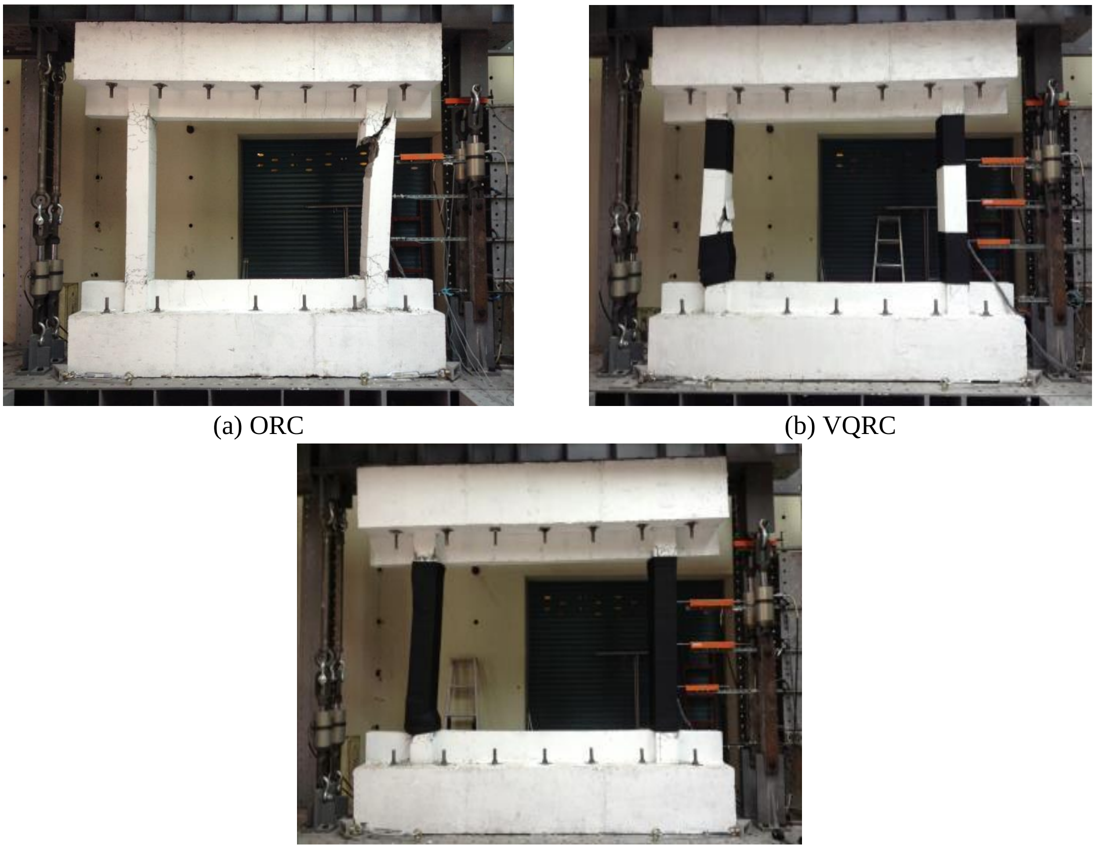
(a) ORC (b) VQRC

(c) VARC

Fig. 11 Final failure mode

The ORC specimen was the reference used to evaluate the performance of the Velcro. The VARC and VQRC specimens were used to evaluate the performance of the Velcro. The Velcro was wrapped at both ends of all columns in the VQRC specimen, and over the entire length of the columns in the VARC specimens. Fig. 10 shows the final deformed shape of all specimens. Critical failure was obtained in the upper plastic-hinge zone of the right RC column (Fig. 11(a)). In case of the VQRC specimen, critical failure was obtained in the lower plastic-hinge zone of the left RC column (Fig. 11(b)). For the VARC specimen in particular (Fig. 11(c)), critical failure was obtained in all plastic-hinge zones of the VARC specimen. The Velcro was delayed or prevented the occurrence of abrupt load drop-down of the RC column, and the failure mode of each specimen was different. In particular, the results for the VARC specimen indicated that the strength of the columns was maintained due to the constraint imposed by the Velcro, even if plastic-hinge motion occurred in the columns. Thus, this appears to have been the final failure mode for the VARC specimen.

4.2 Column behavior

Fig. 12 presents the column height and lateral displacement relationship by displacement ductility factor. The column behavior of all specimens showed ductile and double-curvature behavior before the final load step. The VQRC and VARC specimens achieved a greater number of load-step, than by the ORC specimen. The final load-step of the VARC specimen was larger than that of the others.

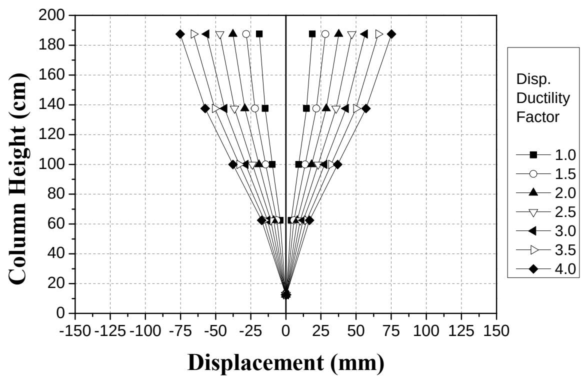

(a) ORC

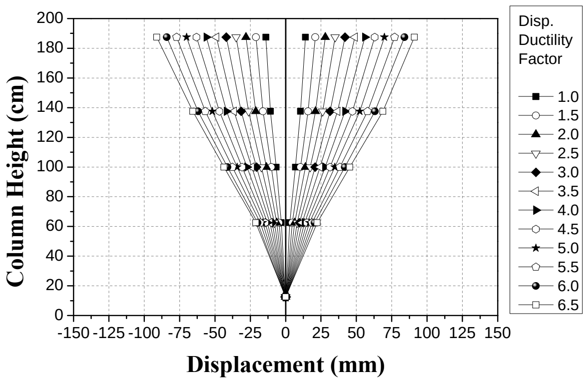

(b) VQRC

Fig. 12 Flexural behavior of columns

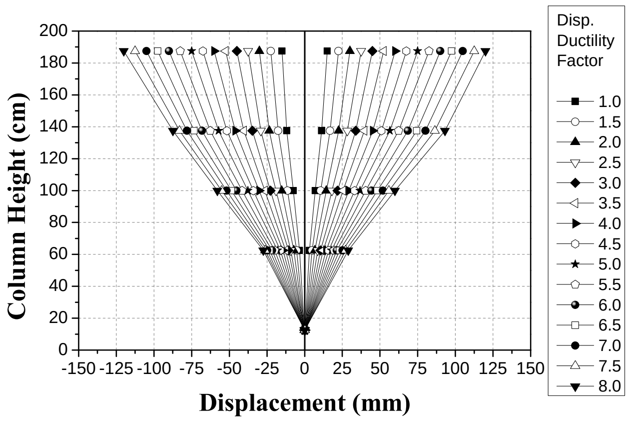

(c) VARC

Fig. 12 Continued

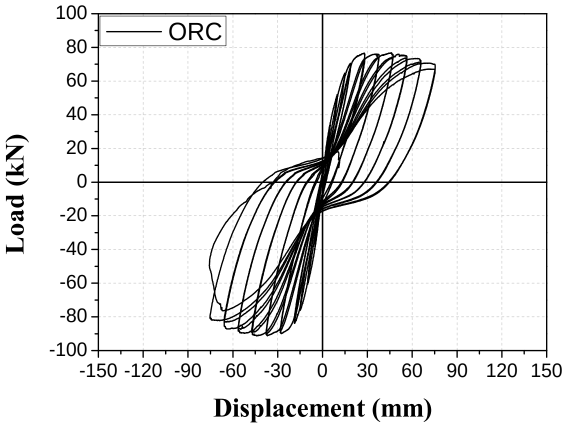

(a) ORC

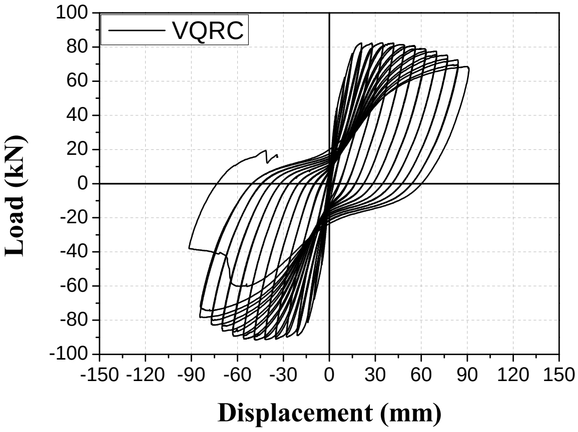

(b) VQRC

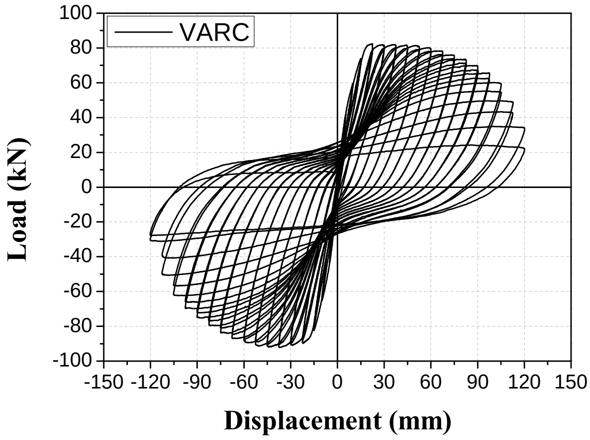

(c) VARC

Fig. 13 Load and displacement relationships

4.3 Strength and displacement

All specimens were tested by the displacement ductility factor. The yield displacements were 18.5 mm, 14.0 mm and 14.9 mm (ORC, VQRC and VARC specimen, respectively). Fig. 13 presents the load and displacement relationships of the specimens tested. The ultimate displacement of the VQRC and VARC specimens (reinforced with Velcro) was larger than that of the ORC specimen, even though the maximum strength of all specimens was almost the same. This means that the Velcro was more effective for increasing the lateral displacement of columns, than for increasing their maximum strength.

In order to compare test results for both strength and displacement of the specimens, an envelope curve was used. Fig. 14 shows the envelope curves for each specimen. The maximum strengths and ultimate displacements of the specimens are summarized in Table 3. The maximum strength of all the tested specimens was almost the same. However, the ultimate displacements of the VQRC and VARC specimens increased. The ultimate displacement of the VQRC specimen was 16% greater than that of the ORC specimen, while the ultimate displacement of the VARC specimen was 26% greater than that of ORC specimen. For Velcro-wrapped specimens, ultimate displacement was increased, whereas maximum strength was almost the same.

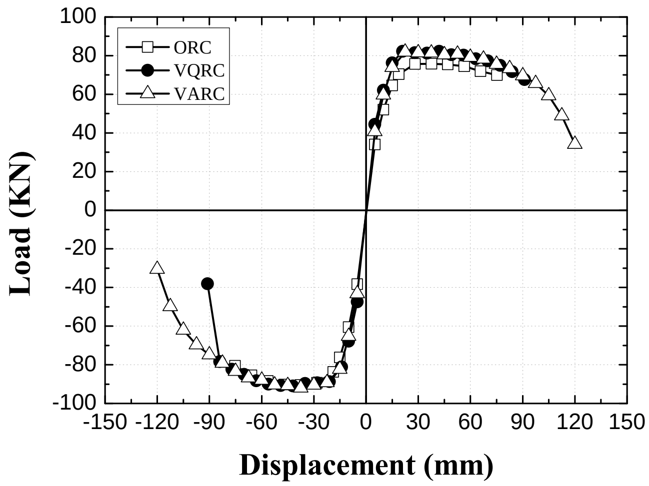

Fig. 14 Envelope curve

Table 3 Experimental test results

Specimen	Max. Strength (kN)		Ratio North (South)	Ultimate Disp.(mm)		Ratio North (South)
	North Direction	South Direction		North Direction	South Direction	
ORC	76.7	91.2	1.00 (1.00)	75.5	69.8	1.00 (1.00)
VQRC	82.5	91.6	1.08 (1.00)	87.9	81.1	1.16 (1.16)
VARC	82.4	92.1	1.07 (1.01)	95.4	86.9	1.26 (1.24)

Table 4 Comparison results of ductility capacity

Specimen	Yield Disp. (mm)	North Direction			South Direction		
		Max. Disp. (mm)	Disp. Ductility (μ)	Ratio	Max. Disp. (mm)	Disp. Ductility (μ)	Ratio
ORC	18.5	75.5	4.08	1.0	69.8	3.77	1.0
VQRC	14.0	87.9	6.28	1.5	81.1	5.79	1.5
VARC	14.9	95.4	6.40	1.6	86.9	5.83	1.6

4.4 Ductility

The displacement ductility capacity was calculated from yield displacement and maximum displacement. The maximum displacement was defined as the displacement at 80% of maximum load. The displacement ductility capacities from the experimental results were summarized in Table 4. The displacement ductility capacity of the VQRC and VARC specimens, which were retrofitted with Velcro, was increased compared to that of the ORC specimen. The increases in the ratios of reinforced specimens were from 54% to 57%. The retrofitting method using Velcro increased not only the ultimate displacement of RC columns, but also their displacement ductility capacity.

4.5 Critical failure mode

The failure mode of the VARC specimen was very different from that of the other specimens. The lateral load was not observed to drop in the VARC specimen. During the test, the behavior of the VARC specimen was very stable, and critical failure occurred over the entire plastic-hinge region of the column. Fig. 15 shows the final failure-shape of the column of the VARC specimen, after removal of the Velcro. Buckling of longitudinal rebar had occurred in the critical area of the column. Crushed concrete pieces were in there, and affected column behavior because of the tightly wrapped Velcro. Velcro prevented unconfined concrete from spalling in RC columns. As a result, the Velcro prevented a dramatic load-drop of the columns, and occurred a number of plastic

(a) Un-spalled concrete at column (b) Crack at joint area

Fig. 15 Critical failure of the VARC specimen

(c) Collapsed plastic hinge zone at column

(d) Local buckling of longitudinal reinforcements

Fig. 15 Continued

hinges of the column. Finally, the final failure mode of the RC-frame structure was changed because of the Velcro.

4.6 Energy dissipation capacity

Fig. 16 show the energy dissipation capacities and accumulated energy dissipation capacities from the experimental results. The accumulated energy dissipation capacities are summarized in Table 5. The accumulated energy-dissipation capacities of the tested specimens were 47.6 kN·m, 97.6 kN·m, and 176.2 kN·m, respectively. The accumulated energy-dissipation capacity of the VQRC and VARC specimens was 2.1 and 3.7 times larger than that of the ORC specimen respectively. The VARC specimen offered an advantage for calculating the energy-dissipation capacity, because it was calculated for each cycle.

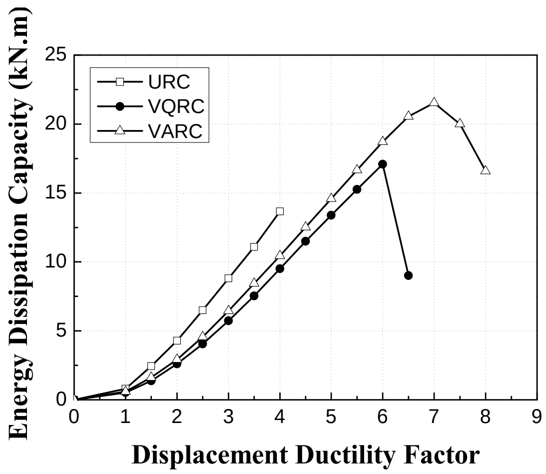

(a) Energy-dissipation capacity

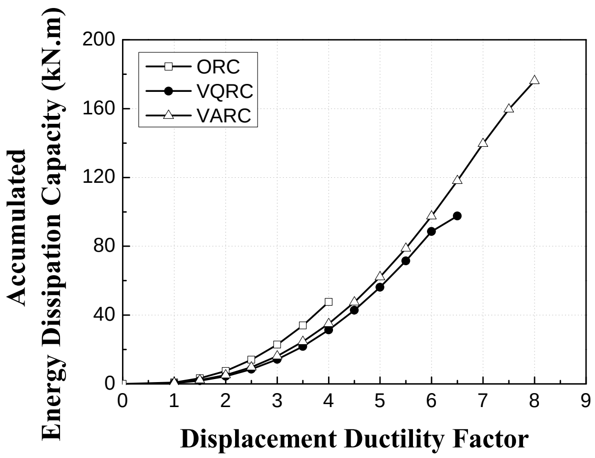

(b) Accumulated energy-dissipation capacity

Fig. 16 Dissipated hysteretic energy-imposed ductility response

Table 5 Accumulated hysteric energy dissipation of specimens.

Specimen	Accumulated Energy Dissipation Capacity (kN·m)	Ratio
ORC	47.6	1
VQRC	97.6	2.1
VARC	176.2	3.7

5. Conclusions

In this study, a seismic strengthening method using Velcro, which is easy and fast to install, was proposed to improve the seismic performance of RC-frame structures. Velcro was prevented concrete spall falling from RC columns. The proposed method was evaluated experimentally using three newly fabricated RC specimens, of which two had Velcro wrapped around their columns.

The reinforcing performance of the Velcro was determined using comparisons of seismic performance, including strength, displacement, failure mode, displacement-ductility capacity and amount of dissipated energy, between the test specimens. As the displacements of the reinforced specimens were increased, the amount of dissipated energy increased drastically. The displacement-ductility capacity of the reinforced specimens also increased. Based on the results, it appeared that the final failure mode of the VARC frame structure was changed. Therefore, the proposed seismic reinforcement method using Velcro, could be used to increase the displacement of RC-columns, and could in theory, change the failure mode of RC-frame structures.

Acknowledgments

This research was supported by a grant (15SCIP-B065985-03) from Smart Civil Infrastructure Research Program (SCIP) funded by Ministry of Land, Infrastructure and Transport of Korean government.

References

Aprile, A, and Feo, L. (2007), “Concrete cover rip-off of R/C beams strengthened with FRP composites”, *Compos. Part B: Eng*., **38**(5-6), 759-771.

Ascione, L. and Feo, L. (2000), “Modeling of composite/concrete interface of RC beams strengthened with composite laminates”, *Compos. Part B: Eng*., **31**(6-7), 535-40.

Ascione, L., Berardi, V.P., Feo, L. and Mancusi, G. (2005), “A numerical evaluation of the interlaminar stress state in externally FRP plated RC beams”, *Compos. Part B: Eng*., **36**(1), 83-90.

Camata, G., Corotis, R. and Spacone, E. (2004a), “Simplified stochastic modeling and simulation of unidirectional fiber reinforced composites”, *Probab. Eng. Mech.*, **19**(1), 33-40.

Camata, G., Spacone, E., Al-Mahaidi, R. and Saouma, V. (2004b), “Analysis of test specimens for cohesive near-bond failure of fiber-reinforced polymer-plated concrete”, *J. Compos. Construct.*, **8**(6), 528-538.

Chai, Y.H., Priestley, M.J.N. and Seible, F. (1991), “Seismic retrofit of circular bridge columns for enhancing flexural performance”, *ACI Struct. J.*, **88**(5), 572-584.

Di Ludovico, M., Balsamo, A., Prota, A. and Manfredi, G. (2008), “Comparative assessment of seismic rehabilitation techniques on a full scale 3-story RC moment frame structure”, *Struct. Eng. Mech.*, **28**(6), 727-747.

Ha, G.J. and Cho, C.G. (2008), “Strengthening of reinforced high-strength concrete beam-column joints using advanced reinforcement details”, *Mag. Concrete Res.*, **60**(7), 487-497.

Kim, J.S., Kwon, M.H., Jung, W.Y. and Limkatanyu, S. (2013), “Seismic performance evaluation of RC columns reinforced by GFRP composite sheets with clip connectors”, *Constr. Build. Mater.*, **43**, 563-574.

Lee, H.H. (2007), “Shear strength and behavior of steel fiber reinforced concrete columns under seismic loading”, *Eng. Struct.*, **29**, 1253-1262.

Limkatanyu, S. and Spacone, E. (2002), “Reinforced concrete frame element with bond interfaces. II: State determinations and numerical validation”, *J. Struct. Eng.*, **128**(3), 356-364.

Matsuda, T., Sato, H., Fujiwara, H. and Higashira, N. (1990), “Effect of carbon fiber reinforcement as a strengthening measure for reinforced concrete bridge piers”, First US-Japan Workshop on Seismic Retrofit of Bridges, Tsukuba Science City, Japan.

Monti, G., Filippou, F.C. and Spacone, E. (1997), “Analysis of hysteretic behavior of anchored reinforcing bars”, *ACI Struct. J.*, **94**(3), 248-261.

Priestley, M.J.N. and Seible, F. (1991), “Seismic assessment and retrofit of bridges”, Report Number: SSRP-91-103, University of California, San Diego, California, USA.

Priestley, M.J.N., Seible, F., Xiao, Y. and Verma, P. (1994), "Steel jacket retrofit of squat RC bridge columns for enhanced shear strength. Part II: Experimental results", *ACI Struct. J.*, **91**(5), 537-551.

Priestley MJN, Seible F and Calvi GM. (1996), *Seismic design and retrofit of bridges*, John Wiley and Sons.

Purba, B.K. and Mufti, A. (1999), "Investigation of the behavior of circular columns reinforced with carbon fiber reinforced polymer (CFRP) jackets", *Can. J. Civil Eng.*, **26**(5), 590-596.

Rousakis, T. (2013), "Hybrid confinement of concrete by FRP sheets and fiber ropes under cyclic axial compressive loading", *J. Compos. Construct.*, **17**(5), 732-743.

Rousakis, T. (2014), "Elastic fiber ropes of ultra high extension capacity in strengthening of concrete through confinement", *J. Mater. Civil Eng.*, **26**(1), 34-44.

Rousakis, T. and Tourtouras, I. (2014), "RC columns of square section-Passive and active confinement with composite ropes", *Compos. Part B*, **58**, 573-581.

Saadatmanesh, H., Ehsani, M.R. and Li, M.W. (1994), "Strength and ductility of concrete columns externally reinforced with fiber composite straps", *ACI Struct. J.*, **91**(4), 434-447.

Saadatmanesh, H., Ehsani, M.R. and Jin, M.R. (1996), "Seismic strengthening of circular bridge pier models with fiber composites", *ACI Struct. J.*, **93**(6), 639-647.

Shimomura, T, Fujikawa, H. and Maruyama, K. (2009), "Modeling of load bearing mechanism of RC column with external continuous fiber rope under reversed cyclic load", *The Second International Conference of International Institute for FRP in Constructon for Asia-Pacific Region*, Seoul, South Korea.

Xiao, Y. and Ma, R. (1997), "Seismic retrofit of RC circular columns using prefabricated composite jacketing", *ASCE J. Struct. Eng.*, **123**(10), 1357-1364.

Xiao, Y. and Wu, H. (2003), "Compressive behavior of concrete confined by various types of FRP composite jackets", *J. Reinf. Plast. Compos.*, **22**(13), 1187-1201.

Xiao, Y., Priestley, M.J.N. and Seible, F. (1996), "Seismic assessment and retrofit of bridge column footings", *ACI Struct. J.*, **93**(1), 79-94.

Yan, Z. and Pantelides, C.P. (2011), "Concrete column shape modification with FRP shells and expansive cement concrete", *Constr. Build. Mater.*, **25**(1), 396-405.

Ye, L.P., Zhang, K., Zhao, S.H. and Feng, P. (2003), "Experimental study on seismic strengthening of RC columns with wrapped CFRP sheets", *Constr. Build. Mater.*, **17**(6-7), 499-506.

CC